PCCP

Accepted Manuscript

ROYAL SOCIETY OF CHEMISTRY

www.rsc.org/pccp

Dissolving Process of Cellulose Bunch in Ionic Liquids: A Molecular Dynamics Study

Yao Li,[a,b] Xiaomin Liu,[*,a] Suojiang Zhang,[*,a] Yingying Yao,[a,b] Xiaoqian Yao,[a] Junli Xu,[a,b] and Xingmei Lu[a]

a Beijing Key Laboratory of Ionic Liquids Clean Process, Key Laboratory of Green Process and Engineering, Institute of Process Engineering, Chinese Academy of Sciences, Beijing, 100190, China.

b College of Chemistry and Chemical Engineering, University of Chinese Academy of Sciences, Beijing 100049, P.R. China.

**sjzhang@ipe.ac.cn, xmliu@ipe.ac.cn*

Abstract

In recent years, a variety of ionic liquids (ILs) were found to be capable of dissolving cellulose and mechanistic studies were also reported. However, there still lack detailed information at molecular level. Here, long time molecular dynamics simulations of cellulose bunch in 1-Ethyl-3-Methylimidazolium Acetate (EmimAc), 1-Ethyl-3-Methylimidazolium Chloride (EmimCl), 1-Butyl-3-Methylimidazolium Chloride (BmimCl) and water were performed to analyze the inherent interaction and dissolving mechanism. Complete dissolution of cellulose bunch was observed in EmimAc, while little change took place in EmimCl, BmimCl and nothing significant happened in water. The deconstruction of Hydrogen bonds (H-bonds) network in cellulose was found and analyzed quantitatively. Synergistic effect of cations and anions was revealed by analyzing the whole dissolving process. Initially, cations bind to the side face of cellulose bunch and anions insert into the cellulose strands to form H-bonds with hydroxyl groups. Then cations start to intercalate into cellulose chains due to their strong electrostatic interaction with the entered anions. The H-bonds formed by Cl^- cannot effectively separate cellulose chain and that is the reason why EmimCl and BmimCl dissolves cellulose more slowly. These findings deepen people's understanding on how ILs dissolving cellulose and would be helpful for designing new efficient ILs to dissolve cellulose.

1. Introduction

Due to the deterioration of global environment and exhaustion of fossil fuels, exploitation and utilization of cellulose, which have much appealing properties as biocompatibility and biodegradability, have been investigated worldwide[1-6]. Cellulose is a polysaccharide with the formula $(C_6H_{10}O_5)_n$, consisting of a linear chain of several hundreds to many thousands of β(1-4) linked D-glucose units[7]. In plants primary cell wall, cellulose chains align parallel to

form flat sheets, and the sheets stack together to form the full three-dimensional crystal structure with a wide range of diameters (2~20 nm) and lengths (0.1~100μm)[8, 9]. The crystal structure has a large complex interaction network. O-H···O hydrogen bonds (H-bonds) of hydroxyl group and near-by oxygen exist between neighbouring glucose units in the same chain (intrachain, I) and different chains (interchain, II)[10-12]. Besides, C-H···O H-bonds form between carbon and bonded hydrogen with the oxygen of hydroxyl oxygen in the cellulose sheets (intersheet, III) above or below[13]. These three types of H-bonds compose a three dimensional interaction network which provides strength and robustness against decomposition[2, 14, 15]. That is the reason why cellulose is not soluble in water or other common solvents[16].

Ionic liquids are defined as liquids composed of ions with the melting point around or below 373K[17]. The unique physicochemical properties for ILs, such as low vapor pressure, good thermal stability and reproducibility[18, 19], have led to numerous applications in catalysis, extraction, electrochemistry, etc[20, 21]. In 2002, Swatloski *et al*.[22] reported that cellulose could be dissolved in 1-Butyl-3-Methylimidazolium Chloride (BmimCl) without derivatization and can also be regenerated by adding water. Since then, studies on the application of ionic liquids (ILs) in biomass chemistry have been widely carried out and many kinds of ILs were found to be able to dissolve cellulose, serving as the reaction medium to functionalize cellulose to make cellulose composite materials[23-27]. Imidazolium, pyridinium, ammonium and phosphonium based cations were observed to dissolve cellulose when paired with a strongly basic, H-bond accepting anion[28-31]. Although using IL as solvent for cellulose still exists problems in cost and recycling[3], elucidating how ILs deconstruct crystalline cellulose and the specific roles of anion and cation in the dissolution process are demanded for exploiting more efficient and economic solvent systems for biomass pretreatment[1, 3, 23].

By using NMR or neutron scattering, Remsing *et al*.[32] and Youngs *et al*.[33] found that the solution of cellulose in IL involved stoichiometric H-bonding between cellulose's hydroxyl protons and chloride ions, indicating that the interaction between the anions and cellulose is the main reason for dissolution while cations may play a minor role. However, the NMR results of Zhang and his co-workers[34, 35] indicated that H-bonds formed between ions and hydroxyl groups of cellobiose, especially the H1 proton in the imidazolium ring, directly interacting with the oxygen of hydroxyls in cellobiose (There is still some debates on the interpretation of the NMR result and experimental design [36]). By investigating the ^{13}C NMR spectra of [phC_1mim]Ac with cellulose, Lu *et al*.[37] implied that acidic protons on the imidazolium rings of the cations form C-H···O H-bond with hydroxyl group of cellulose which is essential for the dissolution process. From another point of view, Lindman *et al*.[38]

suggested that cellulose is obviously amphiphilic and the interaction of cations and glucose ring of cellulose is important for explaining cellulose solubility in ILs.

Molecular simulation could reveal the structure details at atomic level thus plenty of inspiring results about the dissolving mechanism were proposed based on this technology. In the early stage, several molecular dynamics (MD) studies of glucose and cellulose oligomers in ILs were reported[39-44]. Youngs et al.[39, 40] focused on glucose-ILs model system and Liu et al.[41, 42] and Zhao et al.[43, 44] investigated cellulose oligomers in different ILs. All the simulation indicated that anions form strong H-bonds with hydroxyl groups in cellulose while imidazolium rings have a close contact to the polysaccharide. Other researches also paid attention to the effect of additive solvents[45-47]. Zhao *et al*.[45] explained why certain amount of aprotic solvents can improve the solubility of cellulose. Huo *et al*.[46] proposed an indicator named "Pair Energy Distribution" to determine which kind of solvent could dissolve cellulose better. Liu *et al*.[47] put a cellulose crystalline in 1-Ethyl-3-Methylimidazolium Acetate (EmimAc) and found that the methyl hydroxyl groups of dissolved cellulose are mainly in the gauche−trans (gt) conformation, explaining why cellulose II is the major component of the regenerated cellulose from ILs. Some people tried to give a reasonable dissolving mechanism from the perspective of thermodynamics[48-51]. Jarin *et al*.[48] used PTMetaD-WTE approach to study the equilibrium glucose ring structure in BmimCl and $BmimBF_4$, providing new insights of potential energy surface towards the dissolution mechanism. Gross *et al*.[49, 50] studied two extreme states of cellulose in both BmimCl and water. Their results revealed that thermodynamic driving forces of cellulose dissolving are more favorable in BmimCl. Cho *et al*.[51] developed a two-phase model and calculated the Potential Mean Force (PMF) value of peeling a glucan chain from a cellulose microfibril surface in BmimCl and water, and they found the free energy is more favourable in BmimCl.

After all, small cellulose-IL system is indirect and lacks of convincing，thus a lot of scientists have made efforts to simulate larger systems which is more realistic[47, 49-53]. Mostofian *et al*.[52] conducted all-atom MD simulations of a 36-chain cellulose microfibril in BmimCl and found that Cl^- interacts with hydroxyl groups in different cellulose layers and $Bmim^+$ stack preferentially on the hydrophobic cellulose surface, stabilizing detached cellulose chains. By simulating small cellulose bundles solvated in ILs, Rabideau *et al*.[53] proposed a preliminary dissolution mechanism. Anions intensively bind to the hydroxyl groups of cellulose surface, weakening the interaction between cellulose chains. Then due to the opposite charge attraction, cations could intercalate into the cellulose bunches, promoting the different cellulose chains separation.

Although the works mentioned above provide useful knowledge of the dissolving mechanism, but there still remains several questions. Firstly, most polysaccharides can even dissolve in water[54], and crystalline form is the main reason for the stability of cellulose in common solvent[8, 14]. So it is far from enough to study a single chain's behaviour in ILs. Secondly, although several mechanisms were proposed, it still lacks detailed information at atomic level, such as the differences between certain ionic species[43, 44]. Last but not least, in the experiment, it takes several hours to dissolve cellulose completely[1, 23]. Therefore, a long time simulation that reveals the complete dissolution process would be very instrumental to give more direct and detailed evidence for the dissolving mechanisms[52, 53].

To solve the proposed questions, in this work, we made two models of cellulose of 4 and 7 chains separately and carried out MD simulations in EmimAc, EmimCl, BmimCl and water. Complete dissolution of cellulose bunch was observed in EmimAc and validated by analysis of H-bonds. Cations and anions act in a synergistic way to dissolve cellulose. The cations initially bind to the side face of the cellulose bunch surface while anions insert into the bunch and form H-bonds with the hydroxyl groups. As plenty of anions come into the cellulose chains, cations start to intercalate between cellulose chains due to their strong interaction with anions. The large volume of ions provide enough space to separate cellulose chains, thus cellulose dissolution begins. Finally, the effect of solvents and cellulose magnitude are discussed. We hope this work could deepen people's understanding of ILs dissolving cellulose and promote designing new solvent system.

2. Methodology

2.1. Simulation Systems

Two kinds of cellulose bunches of 4 and 7 glucan chains, each with 8 residues, were built based on experimental crystallographic data[14] by a toolkit named cellulose-builder[55]. Only cellulose Iβ structure was constructed since cell wall of higher plant mainly consists of Iβ[56]. Figure 1 illustrates the structure of the glucose units, cations, anions, and two cellulose bunches. Because of the computational limitation, this model was not adopted to a larger cellulose crystal, but these small bunches have the typical features of the realistic cellulose microfibril[53]. Moreover, the behaviour of individual Degree Of Polymerization (DP)=8 chain in EmimAc, 1-Ethyl-3-Methylimidazolium Chloride (EmimCl), BmimCl, and water was studied to do some quantitative analysis. In short, twelve IL-cellulose systems were simulated and the details are listed in Table 1. The following results and discussions are mainly about 7 glucan chain system (7*8). In the 3.5 section, the results of 4 glucan chains (4*8) are represented as complementary and the effect of cellulose magnitude is analyzed.

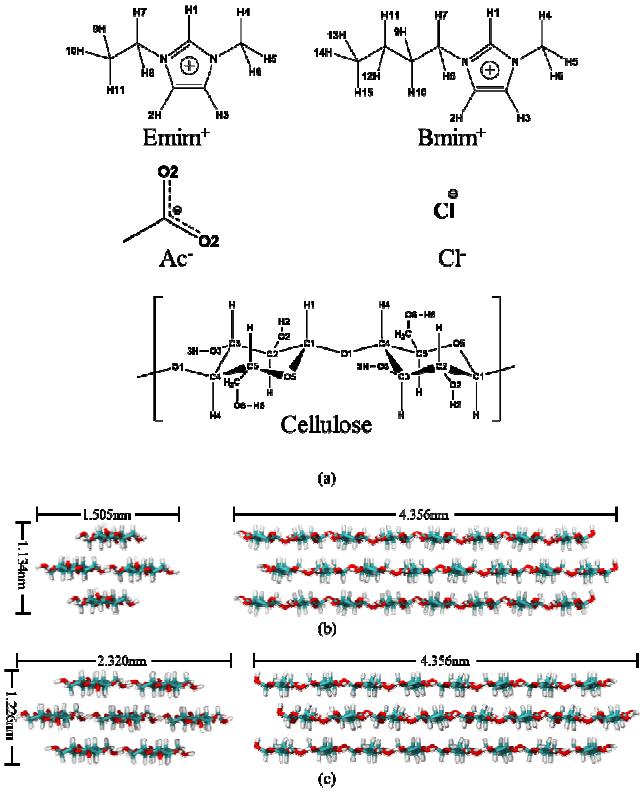

Figure 1. (a) The structure of cations, anions and glucose units used in the simulation. Front and side views of the two kinds of cellulose bunches for 4*8 (b) and 7*8 (c), each of which consisting of 8 glucose units.

Table 1. The components of simulated IL-cellulose systems.

System	Cellulose	Solvent	Number of Solvents	Initial box size(x*y*z/nm)
1	4*8	EmimAc	320	3.74*3.74*6.55
2	4*8	EmimCl	320	3.51*3.51*6.14
3	4*8	BmimCl	320	3.77*3.77*6.60
4	4*8	H_2O	2099	3.24*3.63*6.58
5	7*8	EmimAc	1200	6.84*6.84*6.84
6	7*8	EmimCl	1200	6.49*6.49*6.49
7	7*8	BmimCl	1200	6.43*6.43*6.43
8	7*8	H_2O	5153	4.38*5.51*7.62
9	Single chain	EmimAc	320	3.50*7.00*3.50
10	Single chain	EmimCl	320	3.29*6.57*3.29
11	Single chain	BmimCl	320	3.55*7.09*3.55
12	Single chain	H_2O	3729	4.12*7.22*4.12

The force field parameters for ILs was obtained from Liu's work[57] within the spirit of AMBER framework, while the Glycam06 force field[58] was used for cellulose and the SPC/E model[59] was

used for water. The combination of these force fields is widely used showing good consistency[47, 52]. The isolated ion structures of ILs were optimized using the Gaussian 09 package at the B3LYP/6-31$^+$G* level, and atom charges of ILs (listed in Figure S1) were obtained by fitting the electrostatic potential calculated at the B3LYP/6-31$^+$G* level with restrained electrostatic potential method[60]. Due to the consideration of simulation time and complexity, charge transfer and charge polarization of ILs that occurs in the liquid are neglected in atom charge calculation.

2.2. Molecular Dynamics Simulation Details

The cellulose bunches were solvated in a cuboid box filled with equilibrated ILs, respectively. The cellulose was surrounded by ~2nm solvent on both sides along the polymerization axis direction and by ~3nm perpendicular to the polymerization axis direction. Around 320 (4*8) or 1200 (7*8) ILs were put in the box to provide enough space to dissolve cellulose. All MD simulations were performed and analyzed in Gromacs4.6.5[61]. The Particle-mesh Ewald summation[62] was used in calculation of long-range electrostatics interactions with a cutoff radius of 1.2nm, which was also the cutoff value for VDW interactions. Periodic boundary conditions were used in all directions to mimic a bulk system.

The initial configurations were first minimized by the steepest descent method until the mininum force was under 100kJ/mol•nm to remove the possible coordinate collision. Then the systems were equilibrated for 500ps under *NVT* ensemble with temprature being 373K, corresponding to the experimental dissolution condition[1] (For aqueous solutions it was 300K). Following was a 10ns equilibration dynamics under *NPT* ensemble to equilibrate the solvents. In the above simulations, harmonic restraint potentials were placed on all sugar carbons (force constant 1000 kJ/mol•nm^2) to keep the cellulose bunches around their initial positions. Then the restraints were removed and a production run of 500ns (10ns for single chain) was carried out in the *NPT* ensemble with a 2fs timestep. The simulations in EmimCl and BmimCl were extended to 3μs to compare the difference between BmimCl and EmimCl more clearly. Atomic coordinates, velocities and energies were collected every 20 ps for further analysis. The temperature was maintained by Velocity Rescaling[63] with a time constant of 0.1ps and the reference pressure was 1 bar under Parrinello-Rahman barastat[64] with a time constant of 2.0ps. All covalent bonds were constrained using LINCS algorithm[65].

3. Results and Discussions

3.1. Dissolving process of cellulose bunch

Figure 2 shows the snapshots at different time points of cellulose dissolving in EmimAc (a-f) and water (g-i). In the supporting information, there are two gifs showing the whole disslving

process in EmimAc. The whole cellulose bunch broke up gradually in EmimAc. Finally the chains separated far from each other, implying a completely dissolved state and the single chain was not as straight as before, dispersing in the solvent deviously. Figure 2 g and h show the final configurations in EmimCl and BmimCl. The 7*8 bunches changed a little, still loosely packing together, but they were swelled to a certain degree with single chains tilting up towards the bulk, showing an obvious dissolution trend. The bunch in EmimCl had a more intensive tendency of dispersion as half of the surface chains were peeled from the bunch. As shown in Figure 2 i, only slight fluctuation existed in surface chains and the whole bunch remained the crystall structure in water. Therefore it is concluded that there is no clear trend of cellulose dissolving in water within the 500ns time scale.

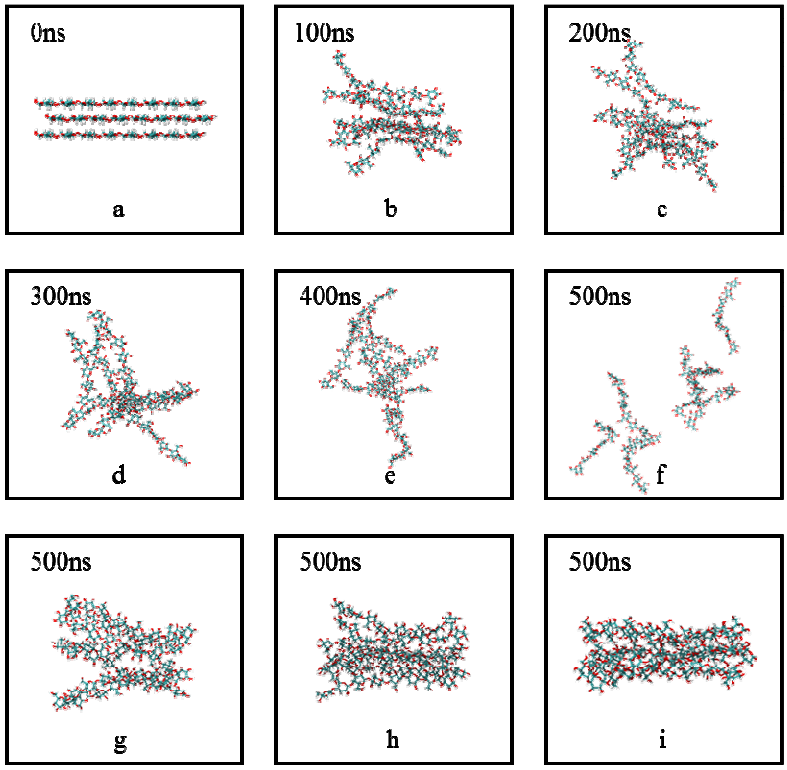

Figure 2. Configuration of cellulose bunch in EmimAc at different time points and final structure in EmimCl, BmimCl and H_2O. Snapshots are taken at (a) 0ns (b) 100ns (c) 200ns (d) 300ns (e) 400ns (f) 500ns in EmimAc and 500ns in (g) EmimCl, (h) BmimCl, (i) H_2O. Solvents are omitted for clarity. Color scheme: red = oxygen; green = carbon; white = hydrogen.

To characterize the stability of cellulose bunch in ILs, we calculated the Root Mean Square Deviation (RMSD) values in atomic positions of cellulose bunch as shown in Figure 3. The curve of 7*8 bunch in EmimAc is the most fluctuant (the black curve), indicating that atom positions changed sharply during the simulation and the cellulose bunch was not stable. For cellulose bunches in EmimCl and BmimCl, curves are more gentle. Only a small rising trend exists, indicating a slight

alteration from their initial structures. Meanwhile, the RMSD curves are consistent with the final conformations of cellulose bunches as illustrated in Figure 2. The black curves for EmimAc are the steepest, indicating the fastest dissolution speed, corresponding to our group's experiments in another work which is to be submitted. The RMSD curve of EmimCl changes a little bigger, so that the final conformation of cellulose bunch in EmimCl is more disordered than that in BmimCl as shown in Figure 2 g and h. In the following sections we will discuss why the cellulose bunch has a slow changing process in EmimCl and BmimCl.

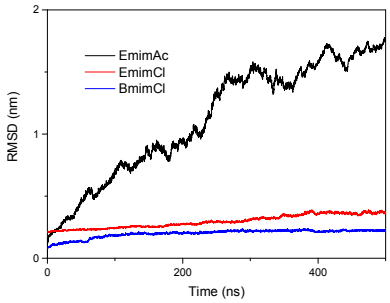

Figure 3. RMSD of cellulose bunches in EmimAc (black), EmimCl (red) and BmimCl (blue).

Our results agree with other published results well. Liu *et al.*[47] observed a significant change of cellulose crystal in EmimAc in 100ns simulation, and Rabideau *et al.*[53] also obtained the same result. But no complete dissociated structure was reported. For the ILs containing Cl^-, Rabideau *et al.*[53] noticed that cellulose crystal did not change much in BmimCl and Mostofian *et al.*[52] found that only the surface chains showed obvious variation in their simulation. Moreover, our group's experimental work indicated that the cell wall of rice hull cell disassembled more rapidly in EmimAc than EmimCl under SEM analysis. Hense the results give a direct evidence and a reasonable explanation for the experimental dissolution speed.

3.2. H-bonds in Cellulose Bunch Dissolving Process

3.2.1 Intrachain and Interchain H-bonds of Cellulose Bunch

Himmel *et al.*[2] proposed that the H-bond network is one of the major reasons for natural resistance of cellulose in plant cell walls to microbial and enzymatic deconstruction. In order to demonstrate the dissolving process of cellulose bunches, tracing the change of H-bond network in cellulose bunches may be a reasonable way. In this work, H-bond in cellulose is classified by intrachain and interchain (Figure 4 a), with a criteria of Donor-Acceptor distance less than 3.5 Å and Hydrogen-Donor-Acceptor angle less than 30°, as shown in Figure 4 b.

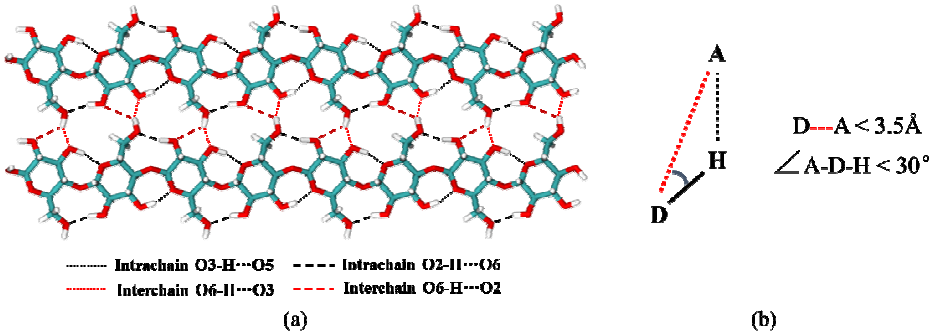

Figure 4. (a) Intrachain (black dotted) and interchain (red dotted) H-bonds and (b) H-bond criteria.

The intrachain and interchain H-bonds of the cellulose bunch in different solvents were investigated as shown in Figure 5. The total hydrogen number of cellulose bunch in the four solvents (Figure 5 a) was about 70 at the beginning time in EmimAc, indicating that a large H-bond network existed in the bunch. However, the intrachain and interchain H-bonds number decreased evidently to a small value. The relatively small number indicates that the cellulose bunch no longer exists as a crystal structure and it disperse in the solvent. Besides, the percentage of H-bonds to its initial value of 7*8 bunch in EmimAc were solely taken out and shown in Figure 6 and the changing process of the four specified H-bonds were shown in Figure 7. It is easy to figure out EmimAc's strong ability to break up the internal H-bonds. There was nearly no interchain H-bond in EmimAc in the final stage. That means there is no close connection between cellulose chains and cellulose bunch dissolves completely in EmimAc. Meanwhile, the interchain H-bonds decreased more rapidly than the intrachain H-bonds. Since O5 exists in the glucose ring, it is easy to form H-bonds with nearby hydroxyl groups, so there are still some intrachain O3-H3⋯O5 H-bonds that ILs cannot break. But the intrachain H-bonds still decreased, which means the single chain become flexible and bendable in the dissolving process.

In EmimCl and BmimCl, since the celluose bunch didn't completely break up, the interchain H-bonds numbers decreased with slow speeds of EmimCl>BmimCl. It seems that longer simulation time is needed for cellulose bunch dissolving in EmimCl and BmimCl, and we are performing longer simulations to track the dissolution process. It was found that the intrachain, interchain and summation H-bonds numbers remained unchanged in water. That may be an evidence that cellulose bunch kept its initial structure in water, consistent with the final conformations and RMSD curves in Figure 2 and 3. Based on the above results, it could be concluded that ILs could break up the H-bond network, while water cannot. H-bond number of cellulose bunch in EmimAc decreases much faster than EmimCl and BmimCl, indicating that EmimAc may dissolve cellulose faster. The experimental data also demonstrate that EmimAc has a faster dissolution rate than EmimCl and BmimCl in dissolving cellulose[66].

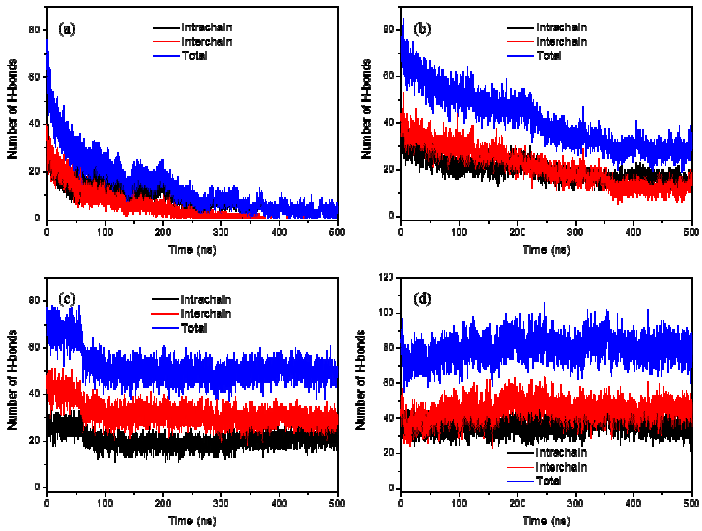

Figure 5. Different 500ns trajectories were used to calculate the number of H-bonds. In all figures, black color represent intrachain H-bond of cellulose bunch and red for interchain, blue for total H-bond. (a) H-bonds number as a function of time of in EmimAc. (b) H-bonds number as a function of time in EmimCl. (c) H-bonds number as a function of time of in BmimCl. (d) H-bonds number as a function of time of in H_2O.

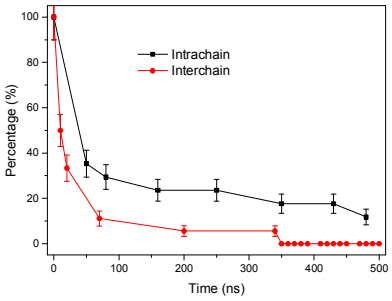

Figure 6. H-bond percentage of initial number. Red for interchain H-bond, black for intrachain H-bond.

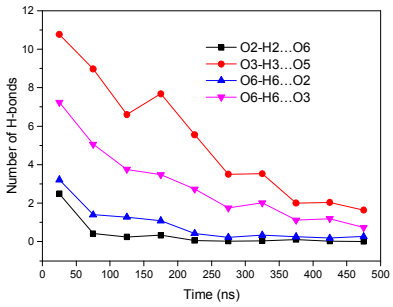

Figure 7. Number of O2-H2⋯O6, O3-H3⋯O5, O6-H6⋯O2 and O6-H6⋯O3 as a function of time, averaged every 50ns. The four kinds of H-bonds refer to Figure 4a.

3.2.2 H-bonds between Cellulose and ILs

The H-bonds formed between anion or cation and cellulose were also taken into consideration. It is widely known that the hydroxyl groups in cellulose glucose rings could form H-bonds with anions easily[32, 41], and the averaged H-bonds number between cellulose and anions in the last 100ns was calculated, which is shown in Figure 8. It can be seen that all the three anions form H-bonds with cellulose hydroxyl groups, in the order of EmimAc > EmimCl > BmimCl. The H-bond distance distributions show that the H-bond distance for Ac^- is much shorter than Cl^- because Van Der Waals radius of Cl^- is larger, and the three kinds of H-bonds share with similar angle distribution.

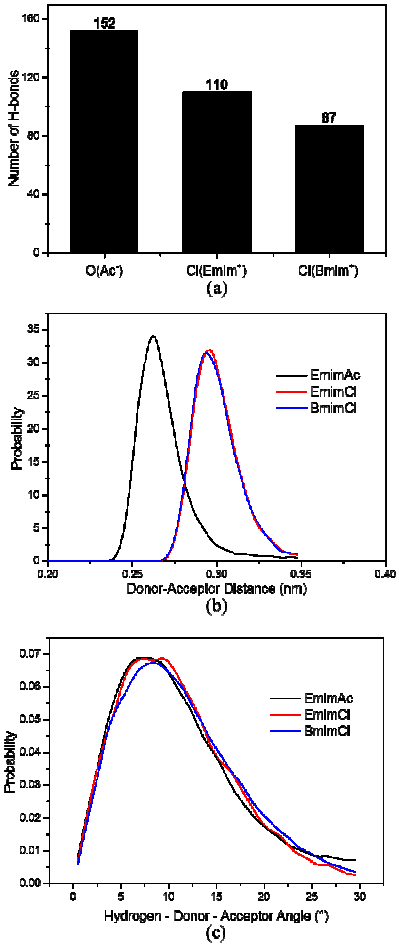

Figure 8. (a) H-bond number between hydroxyl groups in cellulose and anions in the last 100ns trajectories. H-bond distance (b) and angle (c) distributions. EmimAc in black, EmimCl in red and BmimCl in blue.

However, the role of cation in the dissolving process is still controversial[34-36]. Lu *et al.*[37] and Zhang *et al.*[34] proposed that cation maybe another key factor in the dissolving process, for cellulose

solubility varying in ILs composed of different cations and same anion. We divided the hydrogens in cation into three parts (Figure 9) to investigate which part is preferable to form H-bond, and the results are shown in Table 2. Compared with cellulose and anions in Figure 8, the number of H-bonds between cellulose and cations is quite small. The H-bond numbers are in the order of EmimAc >BmimCl> EmimCl. H1, H2, H3 with the most positive charges, form the majority of H-bonds. Dislike the anion-cellulose H-bond, there is no concentrated distribution of cation-cellulose H-bond distance, and the distribution of C-H···O-H H-bonds angle is shown in Figure 10 . The distance should be less than 0.35nm and the angle was ignored. The angles mainly distribute around 50°, compared with H-bonds formed by anion in Figure 8, these H-bonds are relatively weak and could be negligible.

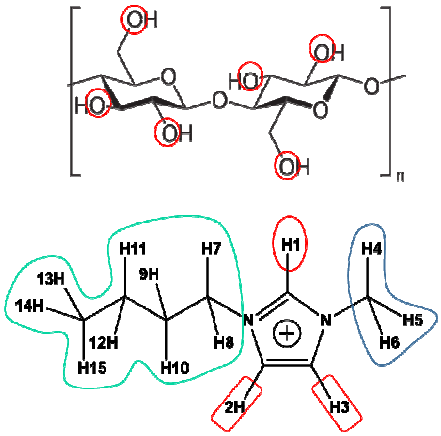

Figure 9. The H-bond donors and acceptors in cations and hydroxyl groups in cellulose.

Table 2. H-bond number of different hydrogens with hydroxyl oxygen in the beginning 100ns.

7*8 bunch	EmimAc	EmimCl	BmimCl
H1 H2 H3	9.11	3.59	7.98
H4 H5 H6	7.54	4.13	4.80
H7-H11(H7-H15)	7.31	4.01	3.34
Total	23.96	11.73	16.12

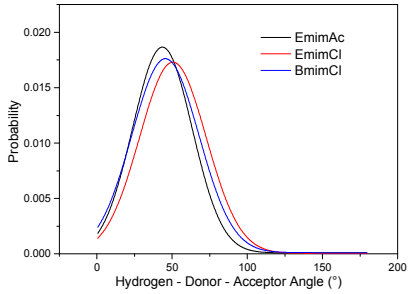

Figure 10. H-bond angle distribution for cation-cellulose H-bond. Black for EmimAc, red for EmimCl and green for BmimCl.

3.3. The synergistic mechanism of Cation and Anion in Dissolving Process

In order to explain the mechanism of ions interacting with cellulose, the dissolving process in EmimAc was taken for analysis. It is found that Ac^- has three typical kinds of H-bond conformations within cellulose chains as shown in Figure 11 a. Each kind of the conformation can provide enough space to separate adjacent cellulose chains. One acetate form H-bonds with only one cellulose chain, leaving another chain facing the non-polarized methyl group, except the fourth conformation. Moreover, no obvious change of the H-bonds number could be found after 350ns from Figure 11 b, which means after a few time for dissolving, cellulose bunch was already detached and cations and anions interacted adequately with single chains. The number of the two kinds of H-bonds, cellulose-cellulose and cellulose-IL, become constant at the same time. That indicates that the cellulose dissolution process is the new cellulose-IL H-bond network replacing the old one[51].

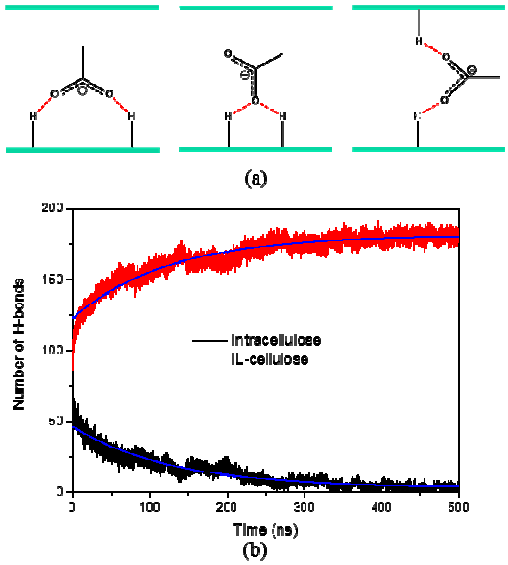

Figure 11. (a) Four kinds of conformations of acetate within two cellulose chains. Captured from 500ns trajectory of cellulose bunch dissolved in EmimAc. (b) H-bonds of cellulose bunch in EmimAc. Red line for number of cellulose-cellulose H-bond, black line for number of cellulose-IL H-bond.

In addition, a DP=8 chain was solvated in three ILs respectively through equilibrium MD simultion to investigate the interaction between ions and the single chain. The interaction energies of single cellulose chain with different cations and anions are listed in Table 3 and the Radial Distribution Functions (RDFs) of different pairs are shown in Figure 12. We find that $Emim^+$ mainly locates around 0.25nm to the hydroxyl group of cellulose, with the interaction energy

around -855.3kJ/mol and Ac^- mainly locates around 0.14-0.2nm, with the interaction energy around -1582.5kJ/mol. Interaction energies of cations are much smaller than those of anions. Energy for cations mainly comes from lennard-jones (LJ) potential while energy for anions mainly comes from coulombic interactions. The charge on cations is more delocalized than on anions because of their larger size. For that reason, electrostatics of anions with cellulose is stronger than that between cations and cellulose. For the same reason, Lennard-Jones interactions of cations with cellulose are stronger because they depend on the contact area and cellulose is more in contact with cations than with anions due to their larger size.

Table 3 Interaction energies of single cellulose chain with different ILs.

E(kJ/mol)	Emi^+	Ac^-	Emi^+	Cl^-	Bmi^+	Cl^-
E_{coul}	-299.57±9.0	-1562.64±15.0	-227.93±3.5	-1553.82±5.0	-74.88±11.0	-1396.72±10.0
E_{L-J}	-555.69±3.5	-19.86±2.0	-639.80±4.0	180.15±2.3	-633.734±1.8	168.384±2.5
E_{total}	-855.26±12.5	-1582.5±17.0	-867.73±7.5	-1373.67±7.3	-708.618±12.8	-1228.34±12.5

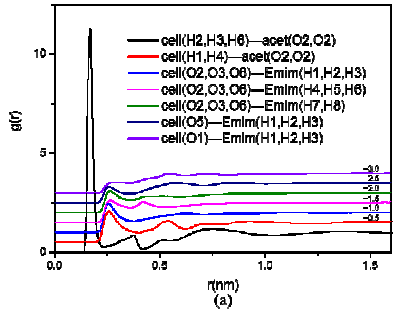

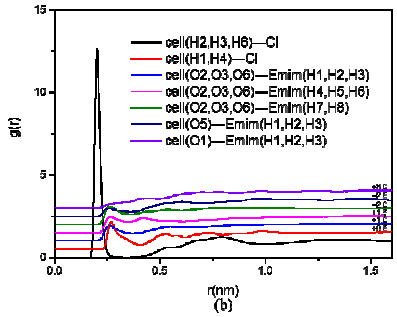

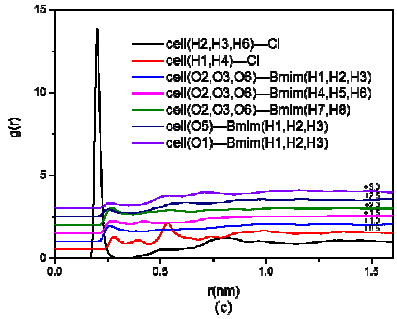

Figure 12. The RDFs of EmimAc (a), EmimCl (b), BmimCl (c) with a DP=8 cellulose chain. The atoms are numbered by the strategy shown in Figure 1 a. Different RDF lines are spaced by 0.5 on the Y axis.

Gross *et al.*[13] proposed that the intersheet interactions are the most robust and strongest component in the interaction network of cellulose. Besides from the massive interchain O-H···O H-bond, strong Van-der-waals interactions also exist between cellulose sheets[38, 47, 52]. In water, glucose rings stack together to avoid unfavorable water-cellulose contacts. But in ILs, the large interaction energy between ions and cellulose maybe favorable. Anions bind with the hydroxyl groups of cellulose surface tightly, loosening the connection between the neighboring cellulose. Then many cations move into the gap of cellulose due to their strong electrostatic interaction with Ac^-. Because cations have strong Van-der-waals interactions interactions with cellulose, it would stack to the single chains instead of other glucose rings and make the solvated chains stable. When enough anions and cations intercalate between two cellulose chains, and the separation process start. Cations and anions act in a synergistic way to dissolve cellulose. Some snapshots were also taken out to investigate the inherent mechanism as shown in Figure 13.

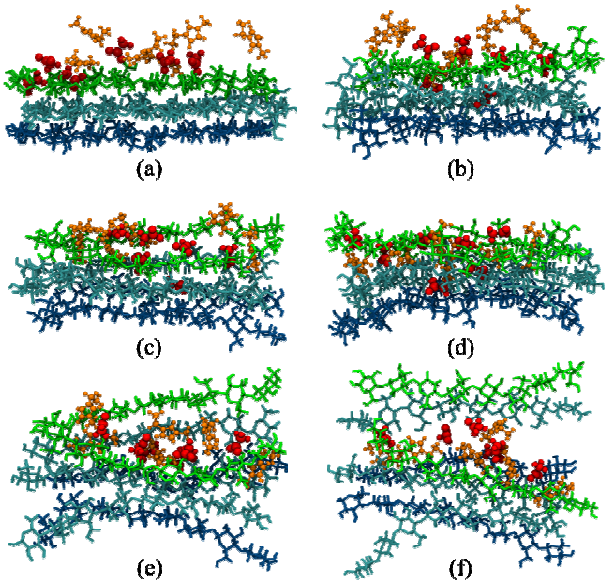

Figure 13. Snapshots of cellulose bunch with selected $Emim^+$ and Ac^- at 1ns (a), 5ns (b), 10ns (c), 20ns (d), 30ns (e) and 50ns (f). Anions are colored red and cations are colored orange.

3.4. Effects of Solvent Structure on Cellulose Dissolution

3.4.1 Effects of Anionic Structure

Cellulose not only has different solubility in different ILs, but also differs in their dissolution rate[23, 66]. Recently, under scanning electron microscope, our group found that EmimAc dissolves

rice shell cell wall more quickly than EmimCl. But there is still little research on why Ac^- is more efficient than Cl^-.

Some snapshots of cellulose chains in EmimAc and EmimCl at 100ns are shown in Figure 14. The entered cations and anions of EmimAc interact with hydroxyl groups in cellulose bunch adequately. Due to the larger ion size, the H-bonds formed by Ac^- with cellulose can effectively loosen the connection between the neighbour cellulose chains and more ions could come in to promote the process. The smaller Cl^- cannot separate cellulose chains to a certain gap and only if there are enough Cl^- intercalating into cellulose, the separation of the chains may begin which would be a slow process. Besides, the data in Table 3 also shows that interaction energy of Ac^- with single cellulose chain is stronger than that of Cl^-. Although the negative charge on Cl (q=-1) is more localized than on the acetate oxygens ($q \approx 0.83$), there are two oxygen atoms in one acetate, and the electrostatic interaction of Ac^- is nearly the same with Cl^-. Moreover, the larger size of Ac^- leads to a stronger Lennard-Jones interaction than Cl^-. As a result, Ac^--cellulose interaction is larger than Cl^--cellulose interaction, which maybe an evidence that Ac^- interacts with cellulose more easily.

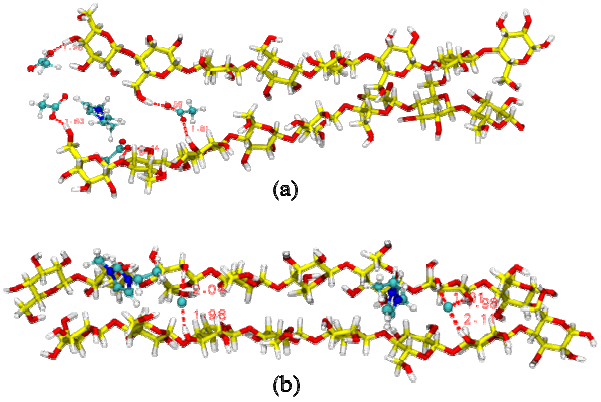

Figure 14. Snapshots of part of cellulose in EmimAc (a) and EmimCl (b) at 100ns.

3.4.2 Effects of Cationic Structure

For the results of the 500ns simulation in EmimCl and BmimCl are not clear enough to show the dissolution trend, we extend the simulation time of 7*8 cellulose bunch in EmimCl and BmimCl to 3μs. The final configurations are shown in Figure 15. In both ILs, the original cellulose structure is disorganized but contacts between chains still exsits especially in BmimCl. The RMSD curves in Figure 16 of the 3μs trajectories shows that the cellulose were dissolving in EmimCl and BmimCl although it was a slow process and the displacement was more sharply in EmimCl. Due to its small size, Cl^- cannot separate the adjacent chains, so the size of the cation maybe a crucial factor. It is more difficult for $Bmim^+$ to penetrate into cellulose bunch because it has a longer alkyl chain. The

charge on the $Bmim^+$ is more delocalized which leads to a weaker electrostatic interaction with cellulose. The data in Table 3 also validates the trend.

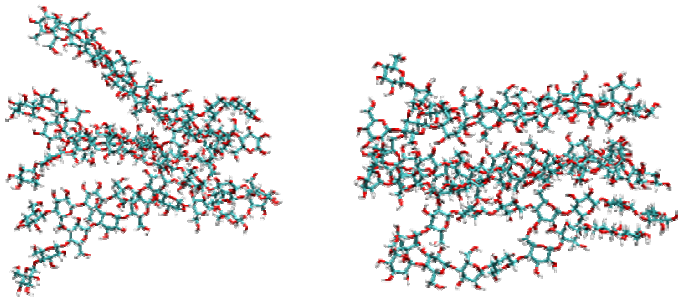

(a) (b)

Figure 15. The final configurations of cellulose bunch in EmimCl (a), BmimCl (b).

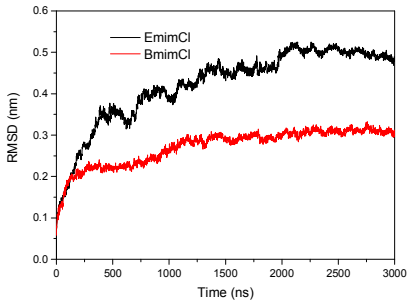

Figure 16. The RDFs of cellulose bunch in EmimCl (black), BmimCl (red).

3.4.3 Difference between ILs and Water

Water has a relatively weak interaction energy with cellulose chain (Table 4), much smaller than ILs (Table 3). Meanwhile, the RDFs in Figure 17 show that there is no concentrated distribution of water around cellulose chains, making isolating single chain difficult.

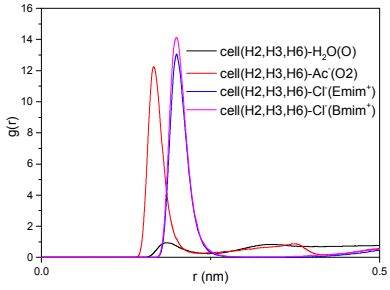

Figure 17. RDFs of the negative charge atoms of different anions around cellulose hydrogens in hydroxyl groups. Water in black, EmimAc in red and BmimCl in blue, EmimCl in green.

Table 4. Interaction energy of water with cellulose chain.

E(kJ/mol)	H_2O
E_{coul}	-1189.21±1.6
E_{L-J}	-248.44±0.6
E_{total}	-1437.65±2.2

3.5. Effect of cellulose magnitude

4*8 cellulose bunch was also studied to investigated whether the bunch magnitude influenced the dissolution process. Figure S2 shows the snapshots of the simulated systems. The RMSD values of 4*8 cellulose bunches were also measured as shown in Figure 18. The tendency of the curves are consistent with the 7*8 results. Since the 7*8 bunch have six surface chains which can be contacted to the solvents adequately, their final RMSD value is bigger than for 4*8 bunch.

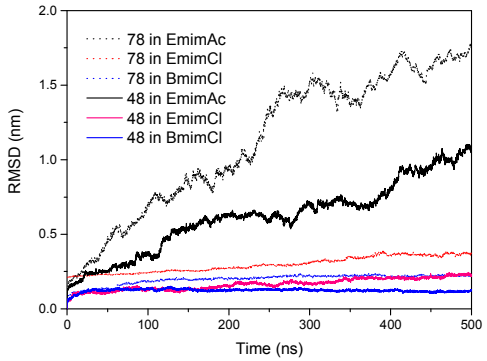

Figure 18. RMSD of 4*8 (solid) and 7*8 (dash) cellulose bunches in EmimAc (black), EmimCl (red) and BmimCl (blue).

The intrachain and interchain H-bonds of 4*8 cellulose bunch dissolving in different solvents were also investigated as shown in Figure S3. The H-bonds of 4*8 cellulose bunch in EmimAc was solely taken out to compare with the 7*8 bunch as shown in Figure 19. The curves of 7*8 cellulose bunch has a much slower speed of decreasing. Therefore, the magnitude of cellulose bunch greatly affect the dissolution speed.

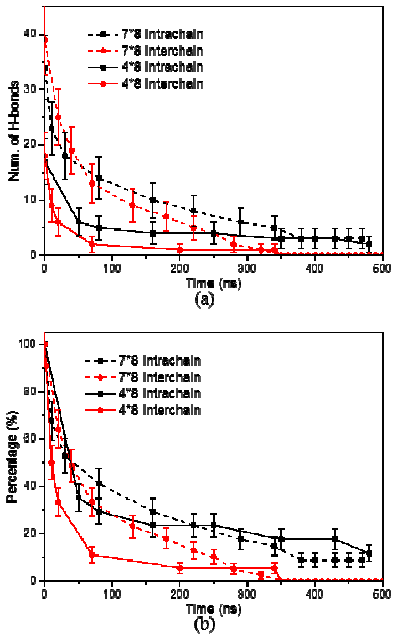

Figure 19 H-bonds of 4*8 and 7*8 cellulose bunch in EmimAc. (a) H-bond number. (b) H-bond percentage of initial number. Red for interchain H-bond, black for intrachain H-bond and solid for 4*8, dash for 7*8.

In Figure 20, the H-bonds of 4*8 cellulose bunch and cellulose-IL H-bonds in EmimAc were compared. After 200ns, there was little change of the number of the H-bonds, meaning that cellulose bunch was already detached. Comparing with the 350ns of 7*8 bunch in Figure 11, it toke much more time to dissolve 7*8 cellulose bunch in EmimAc. The dissolution time length relies on the magnitude of cellulose bunch. For cellulose microfibril in reality, it is much bigger than the simulated model, so it would take a few hours or even longer time to dissolve cellulose using ILs in experiments.

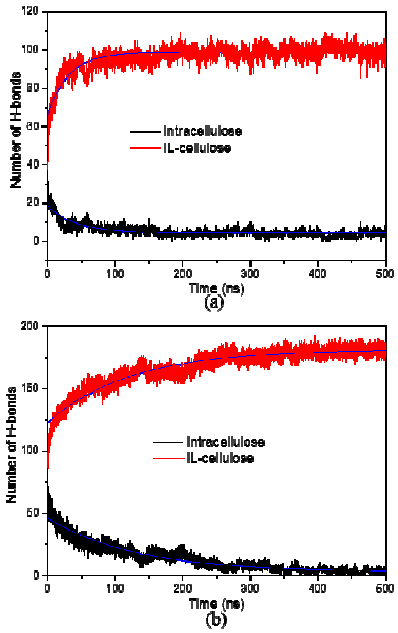

Figure 20. H-bonds of 4*8 cellulose bunch in EmimAc. Red line for number of intracellulose H-bonds, black line for number of cellulose-IL H-bonds.

4. Conclusion

The dissolution of two kinds of cellulose bunches of 4 and 7 glucan chains, each with 8 glucose residues, were investigated by MD simulation. The results demonstrate that the deconstruction of H-bonds network in cellulose happened in ILs. Cations and anions act in a synergistic way to dissolve cellulose. Cations initially bind to the side face of the six-membered rings in the cellulose bunch surface through Van-der-waals interactions while anions insert into the cellulose strands and form H-bonds with hydroxyl group. As more and more anions bind to the cellulose chains, cations start to intercalate into cellulose bunch due to their strong electrostatic interaction with anions and then cellulose dissolution begins. Ac^- can form four different kinds of H-bonds within cellulose chains which can provide enough gaps for cations. Cl^- cannot effectively divide the cellulose chains and this is why EmimAc dissolves cellulose more quickly than EmimCl and BmimCl.

This work provides macroscopic properties and direct phenomenon of cellulose bunch dissolution and gives a synergistic mechanism of ILs interacting with cellulose. The results are complementary to previous work on cellulose-IL interactions and would be inspiring for innovation of new solvent system. While the results shed light on whole events in the dissolution process by ILs, structural changes of large-scale cellulose fiber, which may be more approximated to the reality, remains out of reach due to computational limitation.

Therefore, future research may focus on simulating larger binary systems or identifying distinct interaction patterns[52]. Furthermore, in order to tap the potential of ILs in biomass pretreatment, simulations as well as experiments need to be performed to elucidate the effect of ILs on other components of biomass, such as lignin and hemicellulose[1, 51].

Acknowledgement

We cordially acknowledge the financial support from National Key Basic Research Program of China (2015CB251401), National Natural Science Foundation of China (91434111, 21276255 and 21406230) and Beijing Natural Science Foundation (2142029). We would also like to thank Dr. Kun Dong and Dr. Feng Huo for the helpful suggestion.

References

1. H. Wang, G. Gurau and R. D. Rogers, *Chemical Society reviews*, 2012, **41**, 1519-1537.
2. M. E. Himmel, S. Y. Ding, D. K. Johnson, W. S. Adney, M. R. Nimlos, J. W. Brady and T. D. Foust, *Science*, 2007, **315**, 804-807.
3. M. Gericke, P. Fardim and T. Heinze, *Molecules*, 2012, **17**, 7458-7502.
4. C. E. Wyman, *Trends in biotechnology*, 2007, **25**, 153-157.
5. A. Pinkert, K. N. Marsh and S. Pang, *Industrial & Engineering Chemistry Research*, 2010, **49**, 11121-11130.
6. F. T. Moutos, L. E. Freed and F. Guilak, *Nature materials*, 2007, **6**, 162-167.
7. D. M. Updegraff, *Analytical biochemistry*, 1969, **32**, 420-424.
8. R. M. Brown, *Journal of Polymer Science Part A: Polymer Chemistry*, 2004, **42**, 487-495.
9. S.-Y. Ding and M. E. Himmel, *Journal of Agricultural and Food Chemistry*, 2006, **54**, 597-606.
10. Y. Maréchal and H. Chanzy, *Journal of molecular structure*, 2000, **523**, 183-196.
11. B. Hinterstoisser, M. Åkerholm and L. Salmén, *Biomacromolecules*, 2003, **4**, 1232-1237.
12. K. Tashiro and M. Kobayashi, *Polymer*, 1991, **32**, 1516-1526.
13. A. S. Gross and J.-W. Chu, *The Journal of Physical Chemistry B*, 2010, **114**, 13333-13341.
14. Y. Nishiyama, P. Langan and H. Chanzy, *Journal of the American Chemical Society*, 2002, **124**, 9074-9082.
15. Y. Nishiyama, J. Sugiyama, H. Chanzy and P. Langan, *Journal of the American Chemical Society*, 2003, **125**, 14300-14306.
16. C. Bishop, *Vacuum deposition onto webs, films, and foils*, William Andrew, 2006.
17. R. D. Rogers and K. R. Seddon, *Science*, 2003, **302**, 792-793.
18. K. Dong and S. Zhang, *Chemistry-A European Journal*, 2012, **18**, 2748-2761.
19. K. Dong, S. Zhang and Q. Wang, *Science China Chemistry*, 2015, **58**, 495-500.
20. X. Liu, Y. Zhao, X. Zhang, G. Zhou and S. Zhang, *The journal of physical chemistry. B*, 2012, **116**, 4934-4942.
21. X. Liu, G. Zhou, H. He, X. Zhang, J. Wang and S. Zhang, *Industrial & Engineering Chemistry Research*, 2015, **54**, 1681-1688.

22. R. P. Swatloski, S. K. Spear, J. D. Holbrey and R. D. Rogers, *Journal of the American Chemical Society*, 2002, **124**, 4974-4975.
23. N. Sun, H. Rodriguez, M. Rahman and R. D. Rogers, *Chemical communications*, 2011, **47**, 1405-1421.
24. N. Sun, R. P. Swatloski, M. L. Maxim, M. Rahman, A. G. Harland, A. Haque, S. K. Spear, D. T. Daly and R. D. Rogers, *Journal of Materials Chemistry*, 2008, **18**, 283.
25. T. Heinze, K. Schwikal and S. Barthel, *Macromolecular bioscience*, 2005, **5**, 520-525.
26. J. Xu, X. Yao, J. Xin, X. Lu and S. Zhang, *Journal of Chemical Technology and Biotechnology*, 2014, DOI:10.1002/jctb.4517.
27. J. Xu, X. Yao, Q. Zhou, X. Lu and S. Zhang, *RSC Advances*, 2014, **4**, 27430-27438.
28. A. P. Dadi, S. Varanasi and C. A. Schall, *Biotechnology and bioengineering*, 2006, **95**, 904-910.
29. J.-P. Mikkola, A. Kirilin, J.-C. Tuuf, A. Pranovich, B. Holmbom, L. M. Kustov, D. Y. Murzin and T. Salmi, *Green Chemistry*, 2007, **9**, 1229.
30. D. M. Phillips, L. F. Drummy, D. G. Conrady, D. M. Fox, R. R. Naik, M. O. Stone, P. C. Trulove, H. C. De Long and R. A. Mantz, *Journal of the American Chemical Society*, 2004, **126**, 14350-14351.
31. H. Zhao, G. A. Baker, Z. Song, O. Olubajo, T. Crittle and D. Peters, *Green Chemistry*, 2008, **10**, 696.
32. R. C. Remsing, R. P. Swatloski, R. D. Rogers and G. Moyna, *Chemical communications*, 2006, 1271-1273.
33. T. G. A. Youngs, J. D. Holbrey, C. L. Mullan, S. E. Norman, M. C. Lagunas, C. D'Agostino, M. D. Mantle, L. F. Gladden, D. T. Bowron and C. Hardacre, *Chemical Science*, 2011, **2**, 1594.
34. J. Zhang, H. Zhang, J. Wu, J. Zhang, J. He and J. Xiang, *Physical Chemistry Chemical Physics*, 2010, **12**, 1941-1947.
35. J. Zhang, H. Zhang, J. Wu, J. Zhang, J. He and J. Xiang, *Physical Chemistry Chemical Physics*, 2010, **12**, 14829-14830.
36. R. C. Remsing, I. D. Petrik, Z. Liu and G. Moyna, *Physical chemistry chemical physics : PCCP*, 2010, **12**, 14827-14828; discussion 14829-14830.
37. B. Lu, A. Xu and J. Wang, *Green Chemistry*, 2014, **16**, 1326.
38. B. Lindman, G. Karlström and L. Stigsson, *Journal of Molecular Liquids*, 2010, **156**, 76-81.
39. T. G. Youngs, J. D. Holbrey, M. Deetlefs, M. Nieuwenhuyzen, M. F. Costa Gomes and C. Hardacre, *Chemphyschem : a European journal of chemical physics and physical chemistry*, 2006, **7**, 2279-2281.
40. T. Youngs, C. Hardacre and J. Holbrey, *The Journal of Physical Chemistry B*, 2007, **111**, 13765-13774.
41. H. Liu, K. L. Sale, B. M. Holmes, B. A. Simmons and S. Singh, *The Journal of Physical Chemistry B*, 2010, **114**, 4293-4301.
42. H. Liu, K. L. Sale, B. A. Simmons and S. Singh, *The journal of physical chemistry. B*, 2011, **115**, 10251-10258.
43. Y. Zhao, X. Liu, J. Wang and S. Zhang, *Chemphyschem : a European journal of chemical physics and physical chemistry*, 2012, **13**, 3126-3133.

44. Y. Zhao, X. Liu, J. Wang and S. Zhang, *Carbohydrate polymers*, 2013, **94**, 723-730.
45. Y. Zhao, X. Liu, J. Wang and S. Zhang, *The journal of physical chemistry. B*, 2013, **117**, 9042-9049.
46. F. Huo, Z. Liu and W. Wang, *The journal of physical chemistry. B*, 2013, **117**, 11780-11792.
47. H. Liu, G. Cheng, M. Kent, V. Stavila, B. A. Simmons, K. L. Sale and S. Singh, *The journal of physical chemistry. B*, 2012, **116**, 8131-8138.
48. Z. Jarin and J. Pfaendtner, *Journal of Chemical Theory and Computation*, 2014, **10**, 507-510.
49. A. S. Gross, A. T. Bell and J. W. Chu, *The journal of physical chemistry. B*, 2011, **115**, 13433-13440.
50. A. S. Gross, A. T. Bell and J. W. Chu, *Physical chemistry chemical physics : PCCP*, 2012, **14**, 8425-8430.
51. H. M. Cho, A. S. Gross and J. W. Chu, *Journal of the American Chemical Society*, 2011, **133**, 14033-14041.
52. B. Mostofian, J. C. Smith and X. Cheng, *Cellulose*, 2013, **21**, 983-997.
53. B. D. Rabideau, A. Agarwal and A. E. Ismail, *The journal of physical chemistry. B*, 2013, **117**, 3469-3479.
54. K. Akiyoshi, S. Deguchi, N. Moriguchi, S. Yamaguchi and J. Sunamoto, *Macromolecules*, 1993, **26**, 3062-3068.
55. T. C. Gomes and M. S. Skaf, *Journal of computational chemistry*, 2012, **33**, 1338-1346.
56. D. Klemm, B. Heublein, H. P. Fink and A. Bohn, *Angewandte Chemie*, 2005, **44**, 3358-3393.
57. Z. Liu, S. Huang and W. Wang, *The Journal of Physical Chemistry B*, 2004, **108**, 12978-12989.
58. K. N. Kirschner, A. B. Yongye, S. M. Tschampel, J. Gonzalez-Outeirino, C. R. Daniels, B. L. Foley and R. J. Woods, *Journal of computational chemistry*, 2008, **29**, 622-655.
59. H. Berendsen, J. Grigera and T. Straatsma, *Journal of Physical Chemistry*, 1987, **91**, 6269-6271.
60. C. I. Bayly, P. Cieplak, W. Cornell and P. A. Kollman, *The Journal of Physical Chemistry*, 1993, **97**, 10269-10280.
61. B. Hess, C. Kutzner, D. Van Der Spoel and E. Lindahl, *Journal of chemical theory and computation*, 2008, **4**, 435-447.
62. T. Darden, D. York and L. Pedersen, *The Journal of Chemical Physics*, 1993, **98**, 10089.
63. G. Bussi, D. Donadio and M. Parrinello, *J Chem Phys*, 2007, **126**, 014101.
64. M. Parrinello, *Journal of Applied Physics*, 1981, **52**, 7182.
65. B. Hess, H. Bekker, H. J. Berendsen and J. G. Fraaije, *Journal of computational chemistry*, 1997, **18**, 1463-1472.
66. B. Kosan, C. Michels and F. Meister, *Cellulose*, 2007, **15**, 59-66.